ROCKET MEASUREMENTS OF AURORAL-ZONE ENERGETIC ELECTRONS AT SYOWA STATION, ANTARCTICA

I. CHARACTERISTICS OF ELECTRONS UNDER NO GEOMAGNETIC DISTURBANCE

Masahiro KODAMA, Takashi IMAI, Hajime TAKEUCHI
and Masami WADA

*The Institute of Physical and Chemical Research, Kaga 1-chome,
Itabashi-ku, Tokyo 173*

Abstract: A sounding rocket measurement was made, using a plastic scintillation counter and two proportional counters, of the high energy electrons greater than 40 keV at Syowa Station (L=6.1), Antarctica, in order to search fundamental properties of the energetic electrons under the geomagnetic quiet condition unaccompanied with auroral phenomena. Energy spectra and pitch angle distributions of the electrons were determined as functions of altitude, on the basis of spin-modulated data obtained in the altitude range 70 km–120 km. Peak fluxes were found of the order of $10^3/cm^2 \cdot ster \cdot sec \cdot keV$. The pitch angle distribution over the angle range of 0°–135° peaked at a pitch angle somewhat smaller than 90°, and total integrated fluxes of electrons having pitch angles smaller than 90° were beyond those having pitch angles greater than 90°. Such asymmetry of distribution was established for different energies and altitudes. The exponent of the power law fitting the energy spectrum decreased steadily from 5.7 to 4.0 with increasing pitch angle from 10° to 90°. Fractional contribution of upward and downward electrons is discussed.

1. Introduction

Numerous studies of energization and deposition of the precipitated particles in the auroral zone have been reported so far, particularly by means of rocket and satellite measurements. Most of such studies have concentrated upon essential characters of low energy electrons less than the order of 10^3 eV (*e.g.,* OGILIVIE, 1968; REARWIN, 1971; ARNOLDY, 1974). However, one of the most fundamental problems in magnetospheric physics is the magnetospheric acceleration and precipitation mechanisms of the outer Van Allen energetic particles during geomagnetic disturbances. These energetic particles should be principally responsible for the complicated wave-particle interactions occurring in space close to the

11

earth. They can be detected directly by a small-sized rocket capable of reaching the normal auroral altitude, or indirectly by the atmospheric bremsstrahlung X-rays at balloon altitudes (*e.g.*, Lampton, 1967; Parks, 1970; Lin and Parks, 1974).

A series of rocket experiments to measure >40 keV electrons have been carried out at Syowa Station (69.0°S, 39.6°E, geographic; 69.8°C, 78.5°E, geomagnetic) since 1976. Most of these single-staged sounding rockets, S-210 and S-310, were launched when significant geomagnetic disturbances were observed. But the first rocket was launched at a geomagnetically quiet time, to examine fundamental properties of trapped or precipitated energetic electrons in the auroral zone. This paper presents the observation results of both the energy spectra and the pitch angle distributions obtained in the first flight. Further observation results from successive several flights done under various conditions of disturbance will primarily be discussed as compared with those described here.

2. Instrumentation

The electron detectors used in the first rocket flight, S-210JA-22, launched on 26 January 1976 consisted of a plastic scintillation counter and two high-pressure proportional counters. Specifications and arrangements of these three detectors are shown in Table 1 and Fig. 1, respectively. A photomultiplier tube, RCA C-31016F, for the former viewed four sets of disc-shaped plastic scintillators, each of which was covered by 1.7 mg/cm^2 aluminum foil. An attached collimator with four holes giving a half aperture angle of 20° resulted in the total geometrical factor of 0.076 cm$^2 \cdot$ster.

Table 1. Specifications of electron detectors aboard S-210JA-22 rocket.

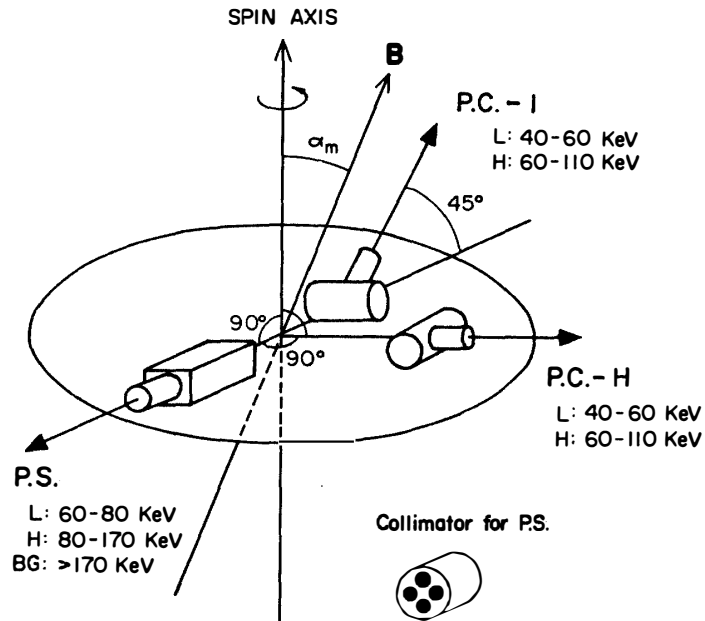|	Effective counter volume	Collimator			Energy band		
		Dimension	Mounting angle	Geometrical factor (cm$^2 \cdot$str)	E_1	E_2	E_3
Plastic scintillation counter (PS)	$6\phi \times 5$ mm	$5\phi \times 13.7$ mm	90°	0.019×4 $=0.076$	60–80 keV	80–170 keV	>170 keV
Proportional counter (PC-H)	$25\phi \times 20$ mm	$6\phi \times 16.5$ mm	90°	0.028	40–60 keV	60–110 keV	None
Proportional counter (PC-I)	//	//	45°	//	//	//	None

Fig. 1. Arrangement of the high energy electron detectors on board the S-210JA-22 rocket. PC and PS mean the proportional counter and the plastic scintillation counter, respectively.

The proportional counter was filled with 2 atms PR gas, mixture of 80% argon and 20% methane, and had a thin mica window of 1.5 mg/cm² in thickness. A collimator was attached so as to give the same aperture angle as in the scintillation counter. The geometrical factor thereby defined is $0.028\ \mathrm{cm^2 \cdot ster}$. Two proportional counters (PC-I and PC-H) were mounted making angles of 45° and 90° from the rocket spin axis, respectively. Viewing directions of the three detectors are as illustrated in Fig. 1.

The counter pulses were separated into two or three channels corresponding to the electron energy bands E_1, E_2 and E_3 as shown in Table 1. The lower threshold energies were determined from the discrimination level in electronic circuit and the thickness of aluminum or mica foil. In this course, energy calibrations were made by using the electron spectrometer with magnet and a variety of artificial radioactive sources, Am^{244}, Ba^{133}, Cd^{109}, Fe^{55} and Sr^{90}.

As seen in Table 1, seven channels of data are available in total. In order to obtain six of them, except E_3, under the limited condition of both the rocket spin rate of ∼2 rps and the available telemeter response of 330 Hz, the six data accumulated during a 50-msec interval were transmitted during the following 50 msec in four digits code. A time interval of 50 msec corresponds to about 36° in spin phase, being comparable with the width of the aperture angle of the detectors. Counting rate in the high energy band E_3 was summed up every one second because of limitation of the telemeter response, and then it was transmitted.

3. Flight Description

A sounding rocket S-210JA-22 was launched from Syowa Station at 0220:00 LT (2330 UT on the preceding day) on January 26, 1976, into an azimuth of 315°(NW) very close to the direction of the local magnetic line of force, and reached a maximum altitude of 119 km. During a couple of days before and after the time of launch, the Syowa magnetometer recorded fairly smoothed time variations whose amplitudes were less than $50\,\gamma$ in horizontal component, and also the 30-MHz riometer showed almost zero absorption. Judging from these facts, it is no doubt that the present flight was carried out during a typical quiet state of magnetospheric condition.

After a removal of the rocket nose cone at 60 seconds after launch, the angle between the rocket spin axis and the local magnetic field changed widely due to a considerable precession motion of the rocket, as can be seen from a solid curve of Fig. 2. Consequently, the horizontal detectors, PS and PC-H, scanned over a
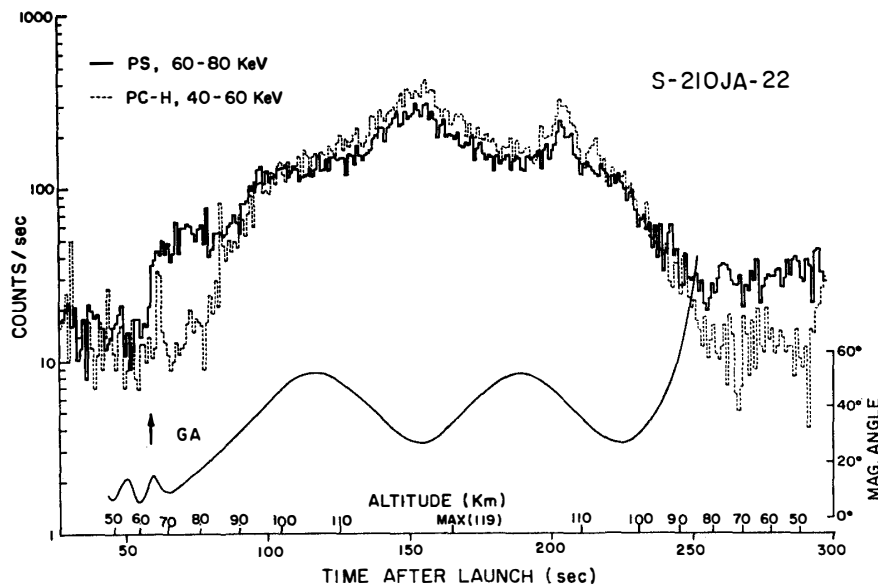

Fig. 2. Time profiles of 1-sec counts of electrons measured by the detectors PS
and PC-H throughout the flight. The angle between the rocket spin axis
and the magnetic line of force is shown by a lower curve. An arrow
indicates the removal of the rocket nose cone.

35°–135° pitch angle range during a precession, whereas the inclined one PC-I covered a 0°–100° pitch angle range.

Fig. 2 also shows the gross character of the energetic electrons sampled throughout the flight, where the 1-sec counts of PS and PC-H detectors in the low energy band E_1 are given. It is seen that the responses of the both detectors

are almost similar, except some discrepancy at roughly 70–80 km which will be discussed in section 6.

4. Reduction of Data

From a time sequence of four digit data transmitted in order, some periodical variation synchronized with the spinning motion was found for all channels of data. During a spin period, there exist two peaks and two valleys, where nearly the same counts refer to the peaks but somewhat different counts to the valleys.

We first assumed that the deeper valley corresponds to the phase of maximum pitch angle. Then it is possible to determine exactly the spin period between
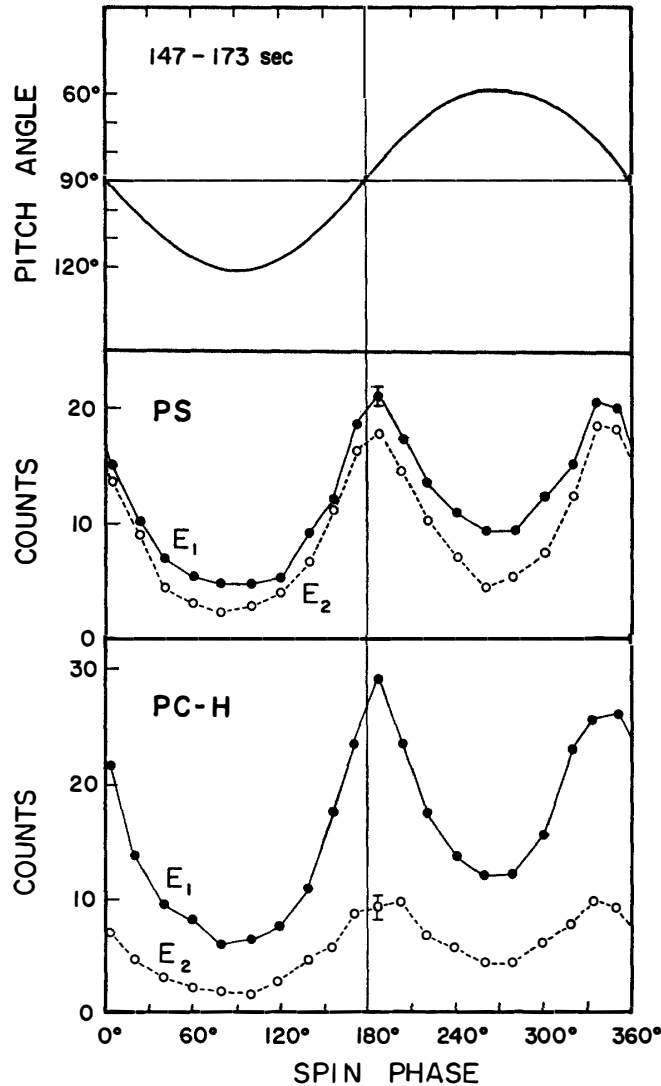

Fig. 3. Changes of the pitch angle (upper) and the electron counts (middle and lower) against rocket spin phase, during a time interval from 147 sec to 173 sec after launch. Both counts from E_1 and E_2 channels are plotted.

the successive deeper valleys by the least square methods, assuming that the spin rate is constant. It was confirmed that thus defined spin phase coincides completely with that based on GA, or, geomagnetic aspect-meter.

Fig. 3 shows one example of such spin-modulated variation obtained during a selected time interval from 147 sec to 173 sec after launch, where counts from the PS and PC-H detectors are plotted every 1/20 subdivision of one spin phase. It should be noted that the two peaks are slightly shifted from 180° and 360°, respectively, regardless of energy.

The pitch angles between the viewing directions of the detector and the magnetic line of force were computed as functions of spin phase and precession angles. The pitch angles thereby obtained near the minimum precession phase are shown in the upper panel of Fig. 3. From comparison between the upper and the middle (or lower), count-pitch angle relation can be deduced easily.

5. Results

In what follows, principal investigations were made of data obtained at altitudes greater than 90 km. Because intensity-time profiles are similar there between the different types of detectors PC and PS, as seen in Fig. 2.

5.1. Pitch angle distribution

In Fig. 4 are shown the counts obtained by the detectors PS and PC-I at 90–100 km and 110–119 km altitude ranges as functions of pitch angle, where
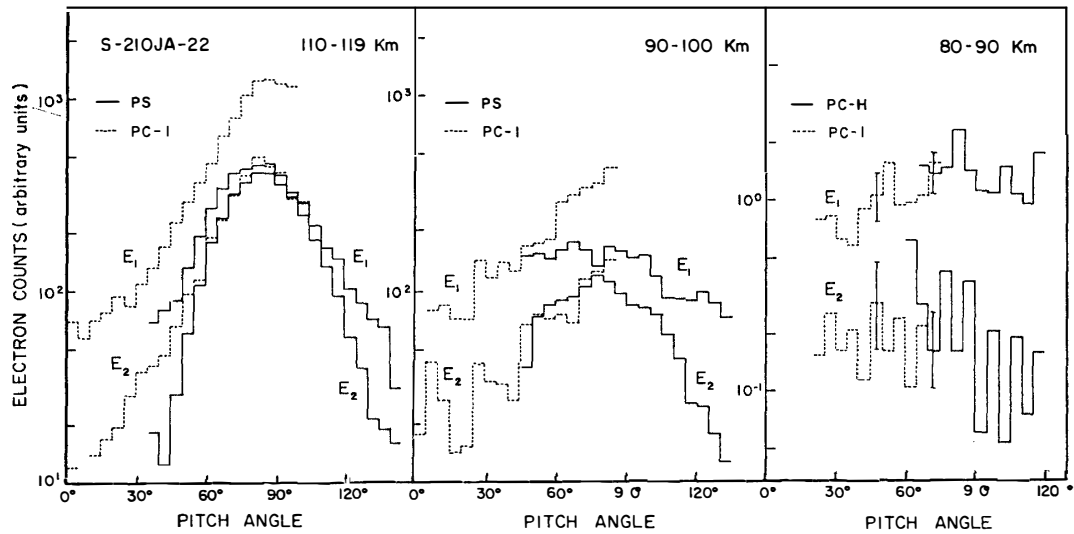

Fig. 4. Electron counts in the energy range E_1 and E_2 versus pitch angles from 0° to 135° : (left) at 110–119 km, (middle) at 90–100 km and (right) at 80–90 km.

two curves for the energy bands E_1 and E_2 are plotted, respectively. Also is shown a part of results of 80–90 km in the right panel. Since the counts from the other horizontal detector PC-H displayed almost the same pattern with those of PS, they are not shown in the left and middle panels. Although the aperture angle of each detector is as large as 36°, it turns out to discriminate the pitch
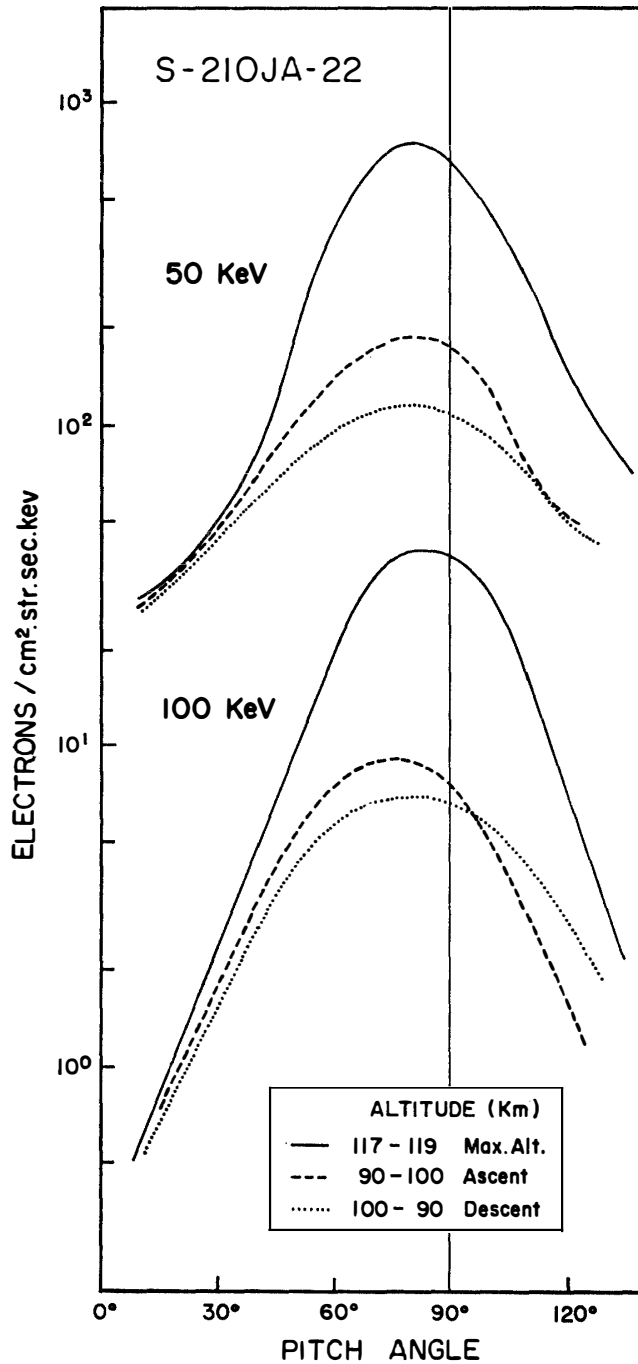

Fig. 5. Pitch angle dependences of fitted fluxes of 50 keV and 100 keV electrons at two different altitudes.

angle by 2° or so, owing to a great number of finely shifted scannings introduced by combination of spinning and precession motions.

It is evident from Fig. 4 that electron fluxes generally peaked around at 90° above 90 km and such pitch angle distribution is obviously dependent of energy and altitude, while the distribution below 90 km is almost isotropic. To demonstrate more clearly such feature, smoothed fits to the data points are shown in Fig. 5, after deducing the energy spectrum which will be described later. Results of 50 keV and 100 keV electrons in the two extreme altitude ranges, 90–100 km and 117–119 km, were sampled. The following interesting characters should be noted:

1) Peak fluxes appeared not in just 90° but in an angle several degrees smaller than 90°, for different energies and altitudes.

2) Total integrated fluxes of electrons having smaller pitch angles than 90° are large compared with those greater than 90°.

3) Amplitude of the pitch angle dependence is enhanced when energy or altitude becomes higher.
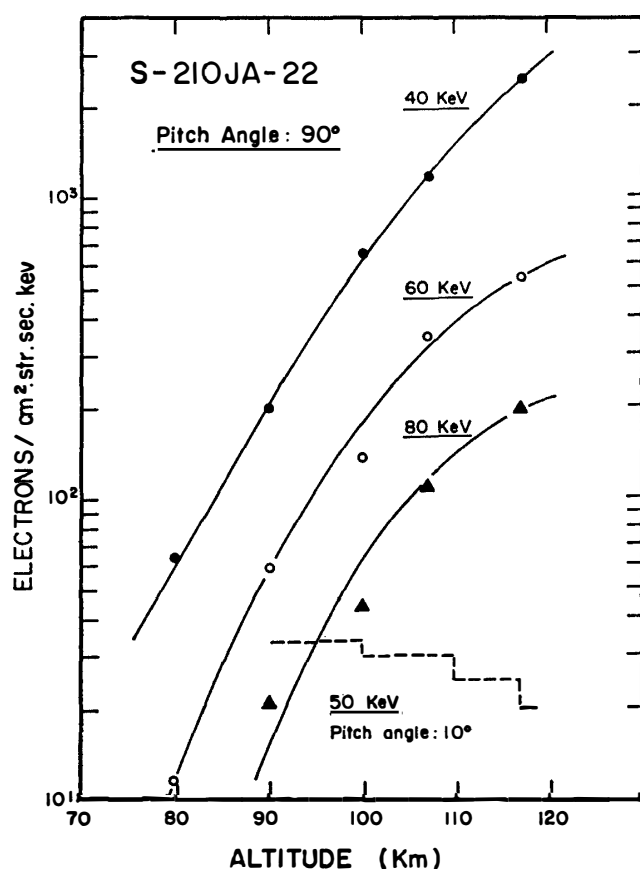
Fig. 6. Altitude dependences of fluxes of electrons with 90° pitch angle for three different energies. A dashed line for 50 keV, 10° pitch angle electrons.

4)   The pitch angle distribution is almost isotropic at altitudes lower than about 90 km.

5.2.   Altitude dependence

Fig. 6 shows fluxes of electrons with 90° pitch angle as a function of altitude, where three different energies were sampled. A general trend of increment of fluxes with increasing altitudes is obvious, and its gradient becomes steeper with decreasing energy. Amplitude of the altitude dependence reduces gradually with smaller pitch angle. In the case of 10° pitch angle, the counts changed slightly with altitude in opposite sense, as indicated by a dashed line in Fig. 6.

5.3.   Energy spectrum

The energy discrimination necessary for deducing the energy spectrum was not so fine and must be based on only four energy channels as shown in Table 1. Therefore, differential fluxes calculated assuming an arbitrary power law exponent
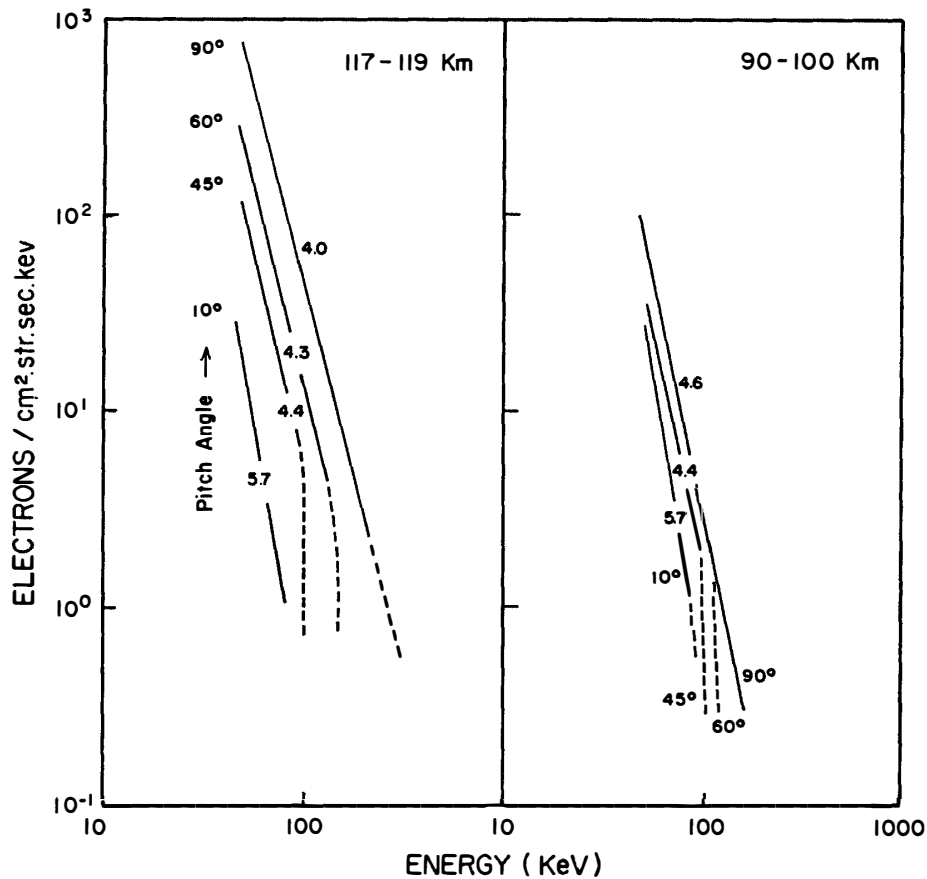

Fig. 7.   Family of fitted energy spectra sorted by pitch angle: (left) at 117–119 km and (right) at 90–100 km.

were compared with six sets of integral fluxes observed in each of the four energy bands. This procedure of analysis was applied separately to selected four pitch angles, 10°, 45°, 60° and 90°. Family of thus fitted energy spectra is given in Fig. 7, where two panels show the spectra from two different altitude ranges.

Maximum flux was found in the case of 50 keV electrons with 90° pitch angle, being $10^3/cm^2 \cdot ster \cdot sec \cdot keV$ at the maximum altitude of 117–119 km, and it reduced by about one order of magnitude at 90–100 km. The spectral exponent varied from 4.0 to 5.7 in correspondence to the pitch angle change from 90° to 10°. For reliable determination of the spectral shape in the higher energy region greater than 100 keV, wherein poor counting statistics and rough discrimination of energy are unavoidable, the least square calculations were made by assuming an upper cutoff on the energy spectrum. As a result, cutoff energies of 100 keV and 130 keV were given for pitch angles of 45° and 60°, respectively. From comparison between two panels of Fig. 7, the altitude dependences of fluxes can be derived for each of the several pitch angles. A part of them was given previously in Fig. 6.

6. Discussion and Summary

As can be seen from the pitch angle distribution of Fig. 5, above 40 keV electrons directly measured by a sounding rocket during no geomagnetic disturbance have concentrated, as a whole, around at 90° pitch angle. This suggests that they are approximately those of trapped-type. It is in contrast with the precipitating-type of low energy electrons less than 10 keV during substorms (Evans, 1967).

We note that asymmetry is pronounced in integral fluxes between the pitch angle ranges smaller and greater than 90°. In general, particles with pitch angles less than 90° mean those coming down along the magnetic line of force into the ionosphere, whereas particles with pitch angles greater than 90° mean those coming up from the lower ionosphere. We define the former as the downward flux and the latter as the upward. Table 2 gives count ratios of the upward electrons to the downward observed at altitudes above 110 km, for each of four data channels. Considering the energy response of each data channel, it is likely that the ratio reduces with increasing energy except the last channel.

In other words, the lower the energy is, the more the upward fluxes increase relatively. This fact may be attributable to developments of scattering and energy dissipation of high energy particles due to atmospheric interactions.

In the case of the PS detector, there is a possibility of a little response to other radiations such as gamma or X-rays. Non-systematic value of the count ratio in the highest energy channel PS-E_2 may suggest such an X-ray contribution.

Table 2. *Count ratios of the upward electrons to the downward electrons.*

Time after launch (sec)	Altitude (km)	Energy channel			
		PC-E$_1$ 40–60 keV	PS-E$_1$ 60–80 keV	PC-E$_2$ 60–110 keV	PS-E$_2$ 80–170 keV
114–213	>110	0.74	0.67	0.65	0.71
148–188	117–119	0.72	0.66	0.61	0.66
188–210	110–117	0.74	0.62	0.67	0.58

Errors of ratios are less than a few percents.

Another possible evidence is seen in some discrepancy between PS and PC time profiles of Fig. 2. Significantly higher fluxes of PS relative to PC are distinct in an approximately 70–85 km altitude range. Such dissimilar response may be due to atmospheric bremsstrahlung X-rays. However, it should be noted that the above enhancement of PS started immediately after removal of the rocket nose cone and no similar enhancement was detected in the E$_2$ energy band of PS. According to the results of ionospheric electron currents observed simultaneously on board the same rocket, the other evidence suggesting possible entry of X-rays was reported (OGAWA, 1977).

Another interesting feature of the pitch angle distribution is a little shift of the peak position from 90° to the smaller. CHASE (1969) calculated that, in the limit of small-angle scattering, an angular distribution that is isotropic above the atmosphere will become peaked in the 50°–70° pitch angle range due to atmospheric interactions. The distributions obtained from the rocket experiment above 200 km revealed the peak value for 60°–65° pitch angles during substorms (REARWIN, 1971). The present results would help to investigate the distribution of particles above the atmosphere.

In Fig. 5, the distributions revealed a certain degree of altitude dependence between the two different levels. However, the distribution during ascent lies nearly above that during descent, despite of the same altitude range. This difference would be caused by gradual shift of the rocket trajectory toward the lower L-values, because the rocket fell at the location of 130 km apart from the launching site toward NW direction. However, it should be noted that the observed distributions are broaden in some degree from the real one owing to the wide aperture angle of the detector, though relative comparisons among them are meaningful.

The altitude dependences of fluxes in Fig. 6 are interpreted qualitatively by taking into account atmospheric interactions of absorption, scattering and energy degradation. For example, the opposite decline of 10° pitch angle electrons against altitude is understood by greater contribution of scattered electrons at

lower altitudes. Also, the softer energy spectrum corresponding to the smaller pitch angle is thought to be due to similar behavior of scattering. Values of the spectral exponents are found to be greater than those during substorms. This fact is reasonably explained by lesser absolute fluxes of energetic electrons, in comparison with high fluxes of 10^4–10^7/cm²·ster·sec·keV during substorms (Evans, 1967). In any way, quantitative explanations are of necessity and importance, as well as strict comparisons with the storm-time characters.

There is an interesting point to be remarked at near 110 km in the descending course. At 200–210 sec after launch, a spike-like intensity enhancement was detected in all of the energy channels, even in >170 keV band. The pitch angle distribution during that time interval did not reveal any particular feature different from the others. Hence, whether this phenomenon is of transient or spatial type is still an open question.

Finally, the following is a summary of characteristics of above 40 keV electrons at 80–120 km during the geomagnetic quiet time;

1) Maximum fluxes are 10^3/cm²·ster·sec·keV being lower by the order of one to four than those during auroral substorms.

2) Fluxes coming down along the local magnetic line of force are about 30% greater than those coming up from the lower ionosphere.

3) Pitch angle distribution is highly dependent of altitude and tends to become isotropic at altitudes less than 90 km.

4) The power law exponent of the energy spectrum varies from 4.0 to 5.7 with the pitch angle change from 90° to 10°, being far greater than that during the disturbances.

Acknowledgments

References

Arnoldy, R. L. (1974): Auroral particle precipitation and Birkeland currents. Rev. Geophys. Space Phys., **12**, 217–231.

CHASE, LEE M. (1969): Energy spectra of auroral zone particles. Ph. D. Thesis, University of California, Berkeley, USA.

EVANS, D. S. (1967): A 10-cps periodicity in the precipitation of auroral-zone electrons. J. Geophys. Res., **72**, 4281–4291.

LAMPTON, M. (1967): Rapid time structure in daytime auroral zone electrons. 48th Annual Meeting, Washington, AGU.

LIN, C. S. and PARKS, G. K. (1974): Further characteristics of the evening energetic electrons decreases during substorms. J. Geophys. Res., **79**, 3201–3205.

OGAWA, T. (1977): private communication.

OGILIVIE, K. W. (1968): Auroral electron energy spectra. J. Geophys. Res., **73**, 2325–2332.

PARKS, G. K. (1970): The acceleration and precipitation of Van Allen outer zone energetic electrons. J. Geophys. Res., **75**, 3802–3816.

REARWIN, S. (1971): Rocket measurements of low-energy auroral electrons. J. Geophys. Res., **76**, 4505–4517.